Early development of direction selectivity in higher visual cortex

Authors: Dallas C. Khamiss[1,2,3], Augusto A. Lempel[1,2,3,4], Brandon R. Nanfito[1,2], Kristina J. Nielsen* [1,2]

Affiliations: [1] Solomon H. Snyder Department of Neuroscience, Johns Hopkins University School of Medicine, Baltimore, MD 21205, USA

[2] Zanvyl Krieger Mind/Brain Institute, Johns Hopkins University, Baltimore, MD 21218, USA

[3]: shared first author

[4] current address: Max Planck Florida Institute for Neuroscience, Jupiter, FL 33458, USA

Corresponding author: Kristina J. Nielsen, knielse4@jhu.edu

Competing interests: The authors declare no competing financial and non-financial interests.

Acknowledgments: This work was funded by NIH EY027853 (KJN) and NIH EY035807 (KJN). We are thankful for O. Garalde, R. Vistein and other members of the Nielsen lab for experimental support, and thank J. Killebrew, W. Nash and W. Quinlan for their technical support.

Abstract

A fundamental aspect of visual motion processing is the computation of motion direction. In ferrets, as in primates, selectivity for motion direction is found both in early cortical stages like the primary visual cortex (V1) and in higher visual areas like primate MT and ferret PMLS. Little is known about how this critical tuning function develops in higher visual cortex. Here, by studying the development of the ferret's motion pathway, we first reveal the surprising finding that direction selectivity develops earlier in PMLS than in V1, contrary to the areas' hierarchical positions. Our data furthermore show that while direction selectivity is sensitive to visual experience in both areas, the sensitivity profile differs between them: Moving stimuli, containing both spatial and temporal cues, are required to promote direction selectivity development in V1, but flashing stimuli that remain stationary spatially are sufficient for direction selectivity development in PMLS. Collectively, our findings reveal that the development of the motion pathway is highly complex when considered at the network level, and does not adhere to a simple feedforward model in which

the development of lower visual areas sets the pace for higher ones. Not only will developmental models need to be updated to include this complexity, characterizing the link between the development of different visual areas will likely also be crucial for understanding the consequences of developmental disorders.

Introduction

Encoding of motion information is a core function of the visual system with high behavioral relevance. Not surprisingly, circuits computing motion have been found in a wide range of species, from flies [1], fish [2] to mammals, including rodents [3–5] and primates (e.g., [6–8]). A particular challenge for motion computations is that they require not just precise processing of spatial cues but also of temporal information, which might be one reason why deficits in motion processing occur in a number of developmental disorders [9]. Because of their behavioral relevance and apparent vulnerability, the development of circuits supporting motion computations is an important topic for investigation.

One of the most fundamental forms of motion processing is the computation of motion direction, which in primates and carnivores predominately occurs in cortex. It is found not just in early stages like the primary visual cortex (V1) [10,11], but also in higher visual areas crucial for motion vision like primate MT [12–14] and ferret PMLS (or PSS) [15,16]. Research on the development of direction selectivity (DS) at the neural level has so far almost exclusively focused on V1 (e.g. [17–20]). As a consequence, very little is currently known about its emergence in higher visual areas like MT or PMLS, leaving a significant gap in our understanding of the development of a core motion computation. Here, we address this issue by systematically following the maturation of DS in ferret V1 and PMLS. Focusing on the same function in both areas also provides the unique opportunity to directly compare the developmental mechanisms at play across the visual hierarchy.

In addition to the time course over which certain functions develop, a second important aspect of visual development is the degree to which it is sensitive to visual information – both its general presence, as well as its specific content. A number of studies have shown that DS development in ferret V1 can indeed be influenced by providing or withholding certain types of visual information [17,21–24]. DS in cat PMLS and monkey MT is also sensitive to altered visual experience during development [25–27]. We have previously shown that the duration of visual experience correlates with the developmental status of motion integration in ferret PMLS [28]. Visual experience therefore also appears to play a role in circuit development in higher motion cortex.

However, all of these studies investigated a single area at a time, and a systematic comparison of the effects of different types of visual experience across the visual hierarchy is lacking. Here, we directly compare the impact of different visual cues on V1 and PMLS development, and use it as a sensitive probe for the developmental mechanisms shaping DS in V1 and PMLS.

In general, our results show a surprising degree of divergence between the two areas, with DS development occurring earlier, and under the influence of different types of visual information, in PMLS than V1. DS development therefore does not simply follow a 'feedfoward' sweep in which higher areas develop after lower ones. This observation provides insights into possible causes for the vulnerability of motion functions to developmental disorders. It also highlights that the visual hierarchy may undergo significant reconfiguration during development, important to consider for models of visual development [29].

Results

<u>After eye opening, DS develops faster in PMLS than V1</u>

DS develops in ferret V1 in the week after eye opening, and matures around postnatal day (P) 37 [17,18]. While we have previously shown that PMLS DS is mature at the same age [28], the time course of maturation has not yet been determined. Here, we systematically tracked PMLS DS development and compared it directly to V1. To this end, we recorded responses to drifting gratings in both areas from P29 (around eye opening) to P52 (young adult). Recordings were performed in anesthetized animals using multi-channel silicon probes, in many cases collecting data from V1 and PMLS simultaneously by recording from 2 probes. All data were collected with the eyes open, irrespective of the natural eye opening state of an animal. Fig. 1B & C show example tuning functions for well isolated single units (SU) in both areas from P30 to P37. As these plots show, we were able to find neurons with reliable visual responses at all ages, which allowed us to quantify tuning properties. The remainder of the analyses in this section will be limited to these visually responsive single neurons (determined using an ANOVA across mean baseline-corrected firing rates for all conditions including the blank with a criterion of $p<.05$; see Methods). The resulting data set sizes are listed in Table 1.

Especially at the youngest ages, tuning functions were often poorly fit with standard direction (or orientation) tuning functions. We therefore quantified DS by computing two different metrics. The first was L_{dir} or 1-DirCircVar, a vector-based metric[30] that takes the entire tuning function into account (see Methods for definition). Importantly, $L_{dir} = 1$ corresponds to high

97 selectivity (responses to a single direction only), while L_{dir} = 0 indicates no selectivity (equal
98 responses to all conditions). This metric is comparable to circular variance (CircVar), commonly
99 used to quantify orientation tuning strength [31]. The second metric used to quantify DS was the
100 direction selectivity index (DSI), which compares only the responses between the preferred
101 direction and the one opposing it (the null direction; see Methods). Results were generally identical
102 between the two metrics, so only the results based on L_{dir} (which is more robust because it is based
103 on the entire tuning curve) are discussed further (see Fig. S1 for the key DSI results). Both L_{dir} and
104 DSI values are indicated for each example neuron in Fig. 1B & C, and suggest a general increase in
105 DS with age in both areas.

106 To more accurately capture the time course of DS maturation and to compare it between
107 areas, we next analyzed DS as a function of age. As a first step, we computed the mean L_{dir} for each
108 individual animal by averaging across all visually responsive PMLS or V1 neurons collected in that
109 animal (results based on the median are comparable; data not shown). This makes it possible to
110 visualize developmental trends without having to group animals by age; it also more clearly shows
111 variability in developmental stage across animals of the same age. Fig. 1D plots these per-animal
112 means as a function of age, with symbol size indicating the number of neurons that passed the
113 selection criterion for each animal. The two horizontal bands correspond to the mean +/- 1
114 standard error (SEM) for animals P40 and older. Consistent with previous data[17,18] from ferret V1,
115 our data show V1 DS to be immature around P30. PMLS DS levels were similarly low at this age. L_{dir}
116 values eventually improved to mature levels in both areas, with some of the improvements
117 occurring very rapidly, as evident by significant changes in DS between animals with a single day
118 age difference. Unexpectedly, this sudden developmental improvement occurred earlier in PMLS
119 than V1 – around P34 for PMLS, P36 for V1. The faster PMLS development continued, in that adult
120 values were reached faster after the initial improvements than in V1. Judging by the overlap
121 between the per-animal mean and the adult range, PMLS matured around P35, but it took V1 until
122 at least P40 to reach this point.

123 This difference between PMLS and V1 development was also apparent when dividing single
124 unit L_{dir} values for each area into 3 age groups used previously for ferret V1 development (collapsing
125 data across animals). The youngest of the 3 groups corresponded to eye opening (P29-32), the
126 second to the phase of rapid DS development (P33-36), and the last sto animals with mature DS
127 levels (P37 and older). Fig. 1E & F plot the L_{dir} distributions for these groups for PMLS and V1. Age
128 had a general effect on the L_{dir} distribution in both areas (Kruskal-Wallis test across all 3 groups:

p<.001 for both areas; full statistics in Table 2). For PMLS, post-hoc rank-sum tests revealed that the P29-32 group deviated from both other age groups (p<.001), which were not significantly different from each other. In V1, on the other hand, the P29-32 & P33-35 groups were not significantly different, but both differed from the oldest group (p<.001).

Since development is obviously dynamic and averaging across age groups cannot capture all trends, Fig. 1G uses an alternate analysis approach to show the relative DS development in V1 and PMLS in more detail. Here, L_{dir} values were binned into age windows of 2 days, combining data across animals. Since in adult animals DS is stronger in PMLS than V1, the comparison of the developmental trajectories between the areas is complicated by the fact that they reach different endpoints. To account for these endpoint differences, we chose to normalize L_{dir} values so that the average L_{dir} in a 2-day window around eye opening (P29 to 30) was set to 0, and the average L_{dir} values in young adults (here, P44-45) was set to 1 (see Methods). V1 and PMLS data were normalized independently, and the normalized L_{dir} values were averaged in each age bin. These normalized time courses again show that PMLS DS development occurred earlier than in V1: PMLS L_{dir} values rapidly increased starting with the P33-34 window, while V1 L_{dir} values remained at the eye-opening level until P35-36. A two-way ANOVA with factors area and age confirmed these observations. For the ANOVA, the age windows used for normalization were excluded (since they are forced to be 0 and 1, respectively), reducing the data to P31 – 39. For these data, the two-factor ANOVA then resulted in a significant effect for age (p<.001), consistent with the general age-dependent change in DS in both areas. Importantly, a significant effect of area (p<.001) and a significant interaction between age and area (p=.003) support differences in DS levels between areas during this time period, which because of the normalization cannot be explained by overall higher DS levels in PMLS, but reflect developmental differences. Further post-hoc rank-sum tests indeed revealed significantly higher normalized L_{dir} values in PMLS than in V1 at P33-34 (p<.001), as well as a trend at P34-35 (p=.02), confirming the earlier development of DS in PMLS (see Table 3 for full test statistics, including the p-values for all non-significant tests). It is worth noting that the time courses in Fig. 1G also suggest that V1 DS development does not just start later, it also takes longer to complete (note the shallower slope of the V1 time course).

At the most fundamental level, high DS requires strong responses to the preferred direction, and weak responses to the opposite (null) direction. To probe some of the mechanisms underlying DS development, we compared the baseline-corrected firing rates evoked by preferred and null direction at different ages. To capture the overall trends, data were divided into the same 3 age

161 groups used for Fig. 1E & F. In both areas, the responses to the preferred stimulus became more
162 robust with age (Fig. 1H & I, see Table 2 for statistics). Kruskall-Wallis tests comparing the 3 age
163 groups were significant for both areas (both p<.001), with significant differences between the P29-
164 32 and the oldest group in both areas (rank-sum tests, both p<.001), as well as differences between
165 the P29-32 and P33-36 groups for V1 (p<.001). The increase in the V1 response to the preferred
166 direction is consistent with previous reports [18]; our data now show that a similar increase occurs in
167 PMLS, but at a later age than in V1.
168 Responses to the null stimulus changed in an area-specific manner as well (Fig. 1J & K). In
169 V1, null direction responses temporarily increased in the P33-36 group, a change that reached
170 significance in comparison to the oldest group, and trended toward significance relative to the P29-
171 32 group (Kruskall-Wallis test: p=.008; rank-sum tests P33-36 versus P37+: p=.006, P33-36 versus
172 P29-32: p=.01). These findings parallel a previous observation of lower V1 null responses after P35
173 than in younger animals[18]. In PMLS, on the other hand, null direction responses gradually
174 decreased with age (Kruskall-Wallis and post-hoc test between the P29-32 and the oldest age
175 group, p<.001; Table 2). This weaker response to the null direction, especially because it was paired
176 with an increase in the preferred direction response, would support better discriminability of the
177 two directions, and points to a role of null direction inhibition especially in the development of
178 PMLS DS (see also Discussion). In summary, our data show earlier and faster DS development in
179 PMLS than V1, in a process that involves area-specific decreases in null direction responses as well
180 as increases in preferred responses in both areas.
181
182 Early PMLS development appears specific to DS
183 Since both V1 and PMLS are tuned for orientation in addition to direction, the development of
184 orientation selectivity (OS) provide the opportunity to assess the areas' relative development along
185 a second tuning dimension, a crucial test for determining whether PMLS develops early in general,
186 or whether the observations made so far are specific for DS development. OS was quantified using
187 two metrics similar to those for DS, a vector-based metric[30,31] called L_{ori} or 1-CircVar, and an
188 orientation selectivity index (OSI). Again, analyses using either metric showed the same results and
189 only L_{ori} data will be shown here (for OSI figures, see Fig. S1).
190 Intriguingly, the relative development of OS in PMLS versus V1 followed a different pattern
191 than that of DS. In V1, consistent with previous reports[32,33], L_{ori} values were low up to P30. Starting
192 with P31, much higher L_{ori} values could be observed, even if there was significant variability across

animals (Fig. 2A). Consequently, dividing the data into the same 3 age groups used for L_{dir} before (P29-32, 33-36, 37+; Fig. 2C revealed significant differences between the P29-32 group and both other groups (Kruskall-Wallis test and both post-hoc rank-sum tests: $p<.01$; Table 4), but not between the two older groups.

In PMLS, OS levels were as low as those found in V1 around P30 (Fig. 2A), with the exception of 2 outliers (one animal contributing 2 neurons, the other 4). Since in all other respects (e.g., their L_{dir} values) these animals were not outliers, their data was included in the OS data set as well. Other than the 2 outliers, OS development in PMLS was delayed relative to V1, with consistent improvements in PMLS L_{ori} values starting only at P34, later than the increase in V1 L_{ori} values. At P34, however, PMLS L_{ori} values immediately assumed their mature levels in a very rapid development, so that OS maturation was complete at the same time point in both areas. Indeed, dividing the PMLS data set into the same 3 age groups as above (Fig. 2B) revealed differences only between the P29-32 age groups and both other age groups, comparable to the results for V1 (Kruskall-Wallis test and both post-hoc rank-sum tests: $p<.001$; see also Table 4).

Given the rapid OS development especially in PMLS, we again turned to binning L_{ori} data into 2-day age windows, normalizing the data to assume 0 and 1 for eye opening and mature levels, respectively, as before (Fig. 2D). Note that the 2 animals with high L_{ori} values around P30 caused the normalized L_{ori} time course for PMLS to initially decrease at P31-32 before rapidly increasing in the next age group. A two-factor ANOVA with age and area (excluding the endpoints used for) was again used to compare development across the areas. It resulted in a significant main effect of age ($p<.001$; see Table 5), consistent with the increase in OS with age. At same time, there was a significant interaction between area and age ($p=.003$), due to significantly higher normalized L_{ori} values in V1 in the P31-32 group (post-hoc rank-sum test, $p<.001$). To rule out possible effects of including the two PMLS outliers in the normalization, we confirmed that a direct comparison of the raw (non-normalized) L_{ori} values for animals aged P31-32 similarly resulted in a significant difference between V1 and PMLS (rank-sum test, $p=.003$). Thus, the onset of OS maturation in PMLS lags behind V1, which in turn highlights that the earlier development of PMLS DS is not due to earlier development of the area in general, but that it reflects processes specific to processing of motion direction.

The relative time courses of DS and OS maturation reveal another very intriguing difference between V1 and PMLS development. Comparing these time courses within each area rather than across areas (see Fig. S2 for a comparison of the normalized L_{dir} and L_{ori} time courses per area), first

225 replicated previous findings of OS development before DS development in V1 [17]. In PMLS, however,
226 our data showed no (or only minimal) delay between DS and OS development (e.g., both
227 normalized time courses show immature levels at P31-32 and significant improvement by P33-34).
228 The normalized L_{dir} and L_{ori} values can again be used to compare the relative development of OS
229 and DS without contamination by overall differences in tuning levels. For V1, a two-way ANOVA with
230 factors age and tuning property on these normalized data resulted in a significant main effect for
231 tuning property ($p<.001$) and age ($p=.006$), but no significant interaction between the factors ($p=.2$),
232 consistent with differences between the two tuning properties that are maintained throughout
233 development (again, the endpoints used for normalization were excluded from the ANOVA). In
234 contrast, in PMLS only the effect of age reached significance, reflecting that DS and OS developed
235 in parallel (age: $p<.001$; tuning: $p=.06$; interaction: $p=.3$). These differences in the sequence of DS
236 and OS development between V1 and PMLS suggest that there might be fundamental differences in
237 the organization of circuits computing direction information in V1 and PMLS (see Discussion).
238
239 Developmental changes in response latency
240 In the marmoset, MT has been shown to develop as early as V1, at least anatomically[34]. This early
241 development involves a transient, direct pathway from the thalamic pulvinar to MT[35,36]. This raises
242 the interesting possibility that early DS development in PMLS is supported by input sources
243 different from those found in adults. Resolving this question will ultimately require anatomical
244 studies. However, response latencies should at least provide some initial insights into network
245 configurations at different ages. As a next step, we therefore decided to analyze the evolution of
246 response latencies in V1 and PMLS with age. Latencies can be quite variable from neuron to
247 neuron. To provide the most robust estimates even at the youngest ages, we increased our sample
248 size by analyzing multi-unit (MU) instead of SU data. Here, MU activity is computed as the
249 thresholded but not spike-sorted activity for each recording channel, ensuring that each spike was
250 only counted on a single channel (see Methods). To be included in the latency data set, MU sites
251 had to meet the same visual responsiveness criterion used for SU above (see Table 1 for the
252 resulting data set size). Additionally, we limited the data set to recording sessions in which data was
253 collected simultaneously for V1 and PMLS so that within-animal comparisons were feasible in all
254 cases. This also minimizes confounds from changes in response dynamics that might be caused by
255 differences in anesthesia state.

For each included MU site, we then determined the onset latency for the site's best stimulus (as the condition evoking the most robust responses). Latencies were computed by binning spikes into 10 ms bins and computing the first bin in which responses exceeded the mean of pre-stimulus baseline activity by two standard deviations, followed by at least two successive bins exceeding baseline activity [37]. Fig. 3A shows raster plots for 3 example V1 MU sites at different ages, as well as 3 example PMLS sites recorded in the same animals. These examples capture two important trends present in the overall data set shown in Fig. 3B: First, latencies in both areas became significantly shorter with age, until very short latencies were reached in adults (median V1 latency across all MU sites: 60ms; median PMLS latency: 70ms). Second, there was a large delay in PMLS responses relative to V1 in young animals. As latencies in both areas gradually improved over the next days, the gap in latencies between the areas ultimately narrowed and became quite small in adults.

Fig. 3C & D plot how these findings play out at the per-neuron rather than per-animal level (see Tables 6 & 7 for full statistics). First, Fig. 3C plots the distribution of latencies for the standard 3 age groups, demonstrating the gradual improvement in latencies with age in both areas (Kruskall-Wallis test across groups per area and all post-hoc rank-sum tests : $p<.001$). Second, Fig. 3D shows how average latencies, computed in 2-day windows (this time without normalization), evolve with age, highlighting the gradual improvement in latencies between P30 and 35 in both areas, as well as the larger delay in PMLS responses in this earlier phase. Indeed, significant differences between V1 and PMLS emerged only for the three age windows falling between P29 and P34 (2-way ANOVA with factors age and area: all main effects and interaction $p<.001$; post-hoc rank-sum tests between areas for P29-30, P31-32, P33-34: $p<.001$), but note that there is still a trend towards larger PMLS latencies for older animals ($p<=.05$ for all subsequent age windows). Finally, we made use of the fact that the data set was limited to cases with simultaneous recordings in V1 and PMLS to test for each animal individually whether V1 and PMLS latencies differed systematically. For this analysis, the PMLS and V1 latency distributions recorded in the same animal were compared against each other using a rank-sum test, and the resulting p-values were Bonferroni corrected by the total number of animals to account for multiple comparisons. Fig. 3E plots the corrected p-values as a function of each animal's age, with the red line indicating $p=.01$. With the exception of one older animal, significant differences between V1 and PMLS latencies using this criterion occurred only before P35.

Taken together, our data show that in addition to age-dependent decreases in response latencies in both areas, extra delays occur in PMLS in young animals, possibly reflecting changing input sources and computational demands with age (see Discussion). Interestingly, for PMLS the maturation of latency coincides with the maturation of DS and OS, while for V1 OS develops before latency matures, and DS thereafter.

Visual experience accelerates DS development in both areas

An important aspect of the development of any visual function is the degree to which it reflects endogenous mechanisms versus the impact of visual experience. In this regard, previous experiments in the ferret have established a highly useful 'training' paradigm that allows controlled tests of the impact of different types of visual experience [21]. In this paradigm, visually naïve animals are exposed to a stimulus of interest for a prolonged period of time (while continuously under anesthesia). Baseline tuning levels like DS are determined before and after stimulus exposure to assess whether the chosen stimulus can exert a measurable influence over neural response properties. For ferret V1, previous studies reported DS increases after exposure to a drifting grating only – exposure to a gray screen was found to be ineffective, as was exposure to a stationary, flashing grating (a grating with temporal modulation of its contrast) [21]. In identifying motion signals as an important cue for V1 DS development, these results demonstrate that the paradigm is a sensitive probe for which types of visual information might influence an area's development. For this reason, we used it here to gain further insights into PMLS DS development.

Experiments using the training paradigm followed the procedures just described. More precisely, we first determined pre-training DS levels in V1 and PMLS in visually naïve animals. We then exposed the animals to a particular stimulus for 8 h. To minimize adaptation, the paradigm was divided into 20 min long stimulation blocks alternating with 10 min of a blank screen (Fig. 4A). Additionally, the stimulation block also consisted of alternating stimulus presentations (5 s) and blank screen periods (10 s). At the conclusion of this training phase, DS levels were again measured in V1 and PMLS and compared to the pre-training levels. Because of the duration of the experiments, we did not attempt to track SU across pre- and post-training measurements. Instead, we assessed DS at the MU level in each case as the more stable measure, reasoning that as electrodes were not moved throughout the experiment, MU activity reflects activity in the same population of neurons before and after exposure (see Methods for inclusion criteria for the training data sets).

As a first test, we investigated the effect of motion cues on DS levels in both areas by showing gratings drifting in one of 2 directions. Directions were chosen to be 180 deg apart from each other so that the same orientation was shown throughout. Using this stimulus set, our data replicated the previous findings of increased V1 DS levels after exposure. Fig. 4B plots the cumulative L_{dir} distribution across MU sites before and after training, demonstrating a significant increase in V1 DS levels after training (rank-sum test, $p<.001$). While this increase is consistent with previous studies, the effect size appears to be significantly smaller in our animals than in those earlier studies [21–24]. A possible explanation for this discrepancy is a difference in the amount of natural visual experience per animal across studies. None of the animals studied here had naturally opened their eyes at the start of the training experiments. In contrast, previous studies included animals of the same age range, but with 1-3 days of visual experience ([22]; van Hooser, personal communication). It is plausible that even brief amounts of natural visual experience can predispose V1 circuits to be able to change more rapidly in response to the training stimuli, therefore resulting in larger effects.

At the same time, since the effect size in our experiments is smaller, there might be a concern that the population data mostly reflects changes in a single animal. In addition to analyzing data across animals, we therefore also used a linear mixed-effect (LME) model to directly control for grouping of data by animal. More precisely, we fit the before- and after-training L_{dir} data with an LME model with a fixed effect for training phase (before/after training), allowing random intercepts and slopes per animal (see Methods and Fig. S3A). On the full data set, the effect of training phase indeed was not significant ($p=.2$). However, 4 out of the 5 animals showed an increase in L_{dir} values after training (Table 8). If the 5th animal (which showed a decrease) is excluded, the effect of training phase becomes significant ($p=.009$).

Importantly, our data show for the first time that exposure to drifting gratings also has a measurable impact on PMLS DS levels. Combined across all animals, L_{dir} levels significantly increased in PMLS with training (rank-sum test, $p<.001$). The LME model similarly returned a significant effect of training phase ($p<.001$), and increases in L_{dir} values for all 5 animals (Table 8). Thus, it appears that drifting gratings contain the necessary information to drive DS development not just in V1, but also in PMLS.

To support this conclusion, it is important to compare the results to the effects of exposing animals to a blank screen for 8 h, to determine whether the observed changes indeed were due to information contained in the stimulus versus a more general effect of unspecific visual stimulation

351 (since the eyes are opened at the start of the experiment) or simply the passage of time. Fig. 4C and
352 S3B plot the L_{dir} changes observed before and after exposure to a homogenously gray screen for 8h
353 for both V1 and PMLS. Based on analyzing the population data irrespective of any per-animal
354 effects, V1 L_{dir} levels actually decreased during this time period (rank-sum test, p=.003). In PMLS, a
355 trend towards higher L_{dir} levels did not reach significance (rank-sum test, p=.01). The LME models,
356 which take per-animal effects into account, showed no significant change in the L_{dir} values for
357 either area (V1: p=.2, PMLS: p=.7), and positive and negative L_{dir} changes occurred with the same
358 frequencies across animals for both areas (Table 8). Thus, for PMLS as for V1, the changes induced
359 by the drifting grating indeed reflected the impact of the particular visual information presented
360 during the training, not unspecific effects.
361
362 PMLS DS development is sensitive to more visual cues than V1
363 The training experiments so far demonstrate that patterened visual experience can impact not just
364 V1 but also PMLS DS development. The next question then is whether certain types of visual
365 information are more important in this process than others. As mentioned above, exposure to a
366 training stimulus lacking motion signals proved ineffective in changing V1 DS levels. To probe
367 whether motion signals are similarly crucial for PMLS DS development, we performed a third set of
368 training experiments, in which animals were exposed to flashing gratings. These gratings were
369 generated by temporally modulating grating contrast between 0% and 100%. Importantly, no
370 contrast reversals were included. This ensured that while the stimulus contrast varied dynamically,
371 the spatial position of the stimulus remained fixed, and no motion cues were provided.
372 The results of these experiments are plotted in Fig. 4D and Fig. S3C. In agreement with the
373 earlier study by Li et al. [21], V1 L_{dir} levels remained unchanged after 8 h of exposure to the flashing
374 grating (rank-sum test, p=.9; LME model: p=.9, 3/6 animals with L_{dir} increases; Table 8). In contrast,
375 the same stimulus was highly effective in PMLS, with significant improvements in L_{dir} at the end of
376 the training experiment (rank-sum test, p<.001, LME model: p<.001, 7/7 animals with L_{dir} increases;
377 Table 8). Our data therefore strongly suggest that in contrast to V1, explicit motion cues were not
378 required for promoting DS development in PMLS. While the flashing gratings are stationary spatially,
379 they nonetheless dynamically changed over time. That means that of the spatiotemporal cues that
380 make up motion information, they at least contained the temporal component. Based on our data,
381 PMLS is sensitive to these temporal cues, while V1 is not (or to a much lesser degree). It remains to
382 be determined whether temporal cues alone are strong enough that a spatially uniform stimulus

383 that changes luminance in time, but lacks spatial information, would nonetheless be sufficient in
384 causing PMLS DS increases.

385 In addition to highlighting the role of different types of visual information, the differential
386 impact of flashing gratings on V1 and PMLS provides a striking example of dissociation in DS
387 development between the two areas reminiscent of the observations during normal development.
388 The training data generally provide an opportunity to further test this idea, because they can be
389 used to ask whether L_{dir} changes induced by the training protocol in V1 are correlated with L_{dir}
390 changes in PMLS. Fig. 4E plots the L_{dir} changes in V1 against the changes in PMLS for each animal
391 (with training effect sizes determined from the per-animal LME models; see Methods). Note that for
392 this plot, we only used animals in which data from both areas was available. The lack of correlation
393 of effect sizes is evident in this figure ($r=-0.09$, $p=0.8$), and supports the notion that DS development
394 in PMLS does not track V1 DS development.

395 As intriguing as the different effects of the flashing gratings on V1 and PMLS are, it needs to
396 be ruled out that the flashing gratings simply fail to activate V1, therefore rendering the stimulus
397 ineffective in driving L_{dir} change. To address this question, we turned to MU responses recorded
398 during the stimulus presentation periods in the training blocks. Responses to flashing gratings were
399 compared against those to drifting gratings, as a stimulus that could generate L_{dir} changes in V1.
400 Fig. 4F plots the average response time courses evoked by both types of stimuli for the two areas
401 (averaging across all blocks and all MU sites in all animals for the 2 training cohorts). These time
402 courses clearly show that flashing gratings did not fail to drive V1, but rather that both types of
403 stimuli evoked reliable activity in both areas. In fact, while peak rates differed between the two
404 areas (Fig. S4), they did not differ between stimulus types (two-way ANOVA with factors area and
405 stimulus type; area: $p<.001$, type: $p=0.1$, interaction: $p=0.3$; Table 10). The major difference
406 between the stimulus types appeared to be the duration of the evoked response (quantified as the
407 time with firing rates above baseline; see Methods), and as a consequence the average rates (Fig.
408 S4, Table 9). More precisely, response durations were significantly shorter for flashing than drifting
409 gratings in both areas (ANOVA with factors area and stimulus type, both main effects and
410 interaction $p<.001$; individual rank-sum tests per area: $p<.001$; Table 9). Interestingly, the difference
411 in response duration was more pronounced in V1 than PMLS. However, if lower V1 drive due to
412 shorter response durations indeed was the reason for a lack of DS change after training with
413 flashing gratings, then response duration should be correlated with the training-induced change in
414 L_{dir}. As is obvious from Fig. 4G, in V1 this is not the case for both stimuli combined or individually

415 (both conditions combined: r=-0.07, p=0.8; drifting: r=-0.7, p = 0.2; flashing: r=-0.3, p = 0.5). The
416 same is the case for PMLS (both conditions: r=-0.6, p=0.04; drifting: r=0.001, p=1; flashing: r=-0.5,
417 p=0.3). Thus, the different effect of exposure to flashing gratings on DS levels in V1 and PMLS
418 cannot simply be attributed to a failure to drive V1 response, but indeed appears to reflect
419 sensitivity to different stimulus attributes across areas.

420

421 **Discussion**

422 A key feature of the experiments presented here is the direct comparison of multiple stages of the
423 ferret's motion pathway. This network-level perspective reveals a complex picture of development,
424 one that does not agree with a simple feedforward sweep in which early stages develop before later
425 ones. Neither are our data consistent with an equally simple reversal of the hierarchy early in life, in
426 which PMLS becomes the primary driver. DS develops earlier in PMLS than in V1, in violation of a
427 strictly feedforward developmental sequence. Yet, PMLS OS does not develop early, and neither
428 does response latency. Paired with different sensitivity to visual cues, it is clear that the
429 developmental status of one area cannot be predicted by that of the other. An important issue to
430 resolve in the future is whether (and which) aspects of V1 and PMLS development indeed proceed
431 independently, and whether any independent development is supported through specific
432 (potentially age-dependent) input channels.

433 The latter is of particular interest because of the anatomical results for primate MT
434 development discussed above. Specifically, based on anatomical data marmoset MT develops
435 structurally as early as V1[34], consistent with our observation of the early functional development of
436 PMLS. This early MT development is supported by a transient pathway providing retinal input to MT
437 through the thalamic pulvinar, different from the standard flow of information through the lateral
438 geniculate nucleus (LGN) and V1 to MT found in adults [35,36]. Whether the input circuits to PMLS
439 undergo similar changes remains to be investigated. The latency data are interesting in this respect:
440 Response latencies in both areas shorten with age, something that has also been observed for
441 monkey V1 and V2 and might suggest general circuit maturation [38]. At the same time, while there is
442 considerable overlap in V1 and PMLS latencies in adults (consistent with data for primate V1 and
443 MT[37,39,40]), up to P35 PMLS latencies are significantly slower than in V1. An intriguing hypothesis then
444 is that the extra delay reflects the cost incurred by driving PMLS activity through different input
445 sources compared to adults (interesting candidates include LGN, pulvinar or superior colliculus).

Since DS is sparse at least in ferret LGN from eye opening on [41,42], the extra delay may also reflect that different input sources require PMLS to compute direction signals *de novo*, rather than relying on 'precomputed' direction signals provided by V1. Finally, it is worth mentioning that around eye opening, PMLS provides the largest fraction of feedback to V1, before closer areas like area 18 become dominant later in life [43]. While further experiments are needed to answer these questions, our data, in conjunction with developmental data from primates, nonetheless strongly argue that development of the visual hierarchy is best described as a dynamic sequence of unique networks that can be configured quite differently from the adult, rather than a gradual, layer-by-layer emergence of the adult hierarchy [29].

One of the unexpected results of our study are the differences in sensitivity to visual cues between V1 and PMLS. Motion computations require the joint processing of spatial and temporal signals. Clearly, around eye opening V1 requires stimuli that provide full spatiotemporal cues to develop DS. It is possible that this changes in slightly older animals, as the role of visual experience switches from instructive (building circuits that reflect the characteristics of the visual input) to permissive (enabling circuit development) around eye opening[24]. Here, animals had not opened their eyes at the time of recording. However, previous studies similarly showing a lack of DS development after exposure to flashing gratings were done in animals with 1-3 days of visual experience[21], therefore suggesting that temporal information in isolation remains ineffective even after visual experience switches to a permissive role. In PMLS, though, the same purely temporal inputs are sufficient in driving DS development, and at least for the specific stimulus properties and animals studied here, might actually be more effective than stimuli with joint spatial and temporal information. On the one hand, this difference in sensitivity could mean that altered visual experience during development could have very different consequences for PMLS and V1 function. On the other hand, it is interesting to speculate about what this sensitivity to temporal cues means for the impact of normal visual experience on PMLS before eye opening. Previous studies have found that reliable visual responses can be recorded in ferret LGN and V1 starting around P17[44,45]. At these ages, ferret kits have been found to make scanning head movements from side to side[45], and at least based on neural responses, the corresponding visual signals, even through the closed eye lids, contain enough structure to result in measurable OS and DS[44]. Nonetheless, the filter applied by the eye lids will likely remove spatial structure to a much larger degree than temporal transients. Thus, natural input before eye opening might contain more of the relevant cues for PMLS than V1 DS development.

478 In addition to these insights into visual hierarchy development, our data may also provide
479 valuable clues regarding motion processing in adult cortex. One important observation in this
480 respect is the relative developmental time course of OS and DS. In V1, we and others observe OS
481 development before DS[17,18]. At least in the ferret, this sequence is reflected in the functional
482 organization of the area: Orientation maps develop first, and show minimal discontinuities (singular
483 points or pinwheels) [17,33,46]. The later developing direction maps are then constrained by the existing
484 orientation maps. As a consequence, they are nestled inside the orientation maps, with each
485 orientation column split into subregions selective for opposite directions of motion (that share the
486 same orientation). As a result, the discontinuities for the direction map take the form of linear
487 fractures at which directions shift by 180 deg [46]. In PMLS, DS and OS mature at the same time. It is
488 therefore possible that the functional architecture is optimized for direction rather than orientation,
489 a question to be resolved in future imaging studies. In monkey MT, extracellular recordings show
490 that neighboring neurons either have very similar direction preferences or differ by nearly 180 deg [47],
491 which would be most consistent with a direction map with linear fractures. Indeed, optical imaging
492 from owl monkey MT shows orientation and direction maps very similar to those found in ferret V1
493 [48]. Yet, recent two-photon data from the marmoset reported predominantly smooth changes in
494 direction preference, rather than sudden 180 deg reversals, at least at the scale of several hundred
495 micrometers [49]. Whether PMLS/MT organization is optimized for direction or orientation therefore
496 remains an open question.
497 Another observation of interest for adult PMLS function is the fact that concurrent with the
498 increase in DS, the response to the null direction decreases. Null direction inhibition is thought to
499 play a role in the generation of DS in primate MT [50–52], and we have suggested the same might be the
500 case in ferret PMLS [16]. While the anatomical and functional development of inhibitory neurons in
501 ferret V1 has received some attention (e.g., [20,53–55]), there are currently no comparable data for
502 PMLS. Further studies are therefore necessary to resolve whether the decreased null direction
503 response is indeed the consequence of the development of selective inhibition (rather than e.g. a
504 change in feedforward drive).
505 Finally, the complex network-level development we observed will be important to consider
506 in the context of both developmental disorders and plasticity mechanisms in the adult brain. Early
507 development, paired with sensitivity to a broad range of visual cues, likely means increased
508 vulnerability to disruptions of normal development early in life – consistent with the observation
509 that motion vision is impaired in a range of developmental disorders (see e.g. [9,29] for reviews). On

510 the other hand, the circuit mechanisms that support at least the early DS development may still be
511 available for reactivation later in life and provide mechanisms for phenomena like blindsight [56,57] or
512 the ability to regain some visual function after V1 stroke through training on a motion task [58].
513
514
515 **References**

516 1. Borst, A. & Groschner, L. N. How Flies See Motion. *Annu. Rev. Neurosci.* **46**, 17–37 (2023).
517 2. Bollmann, J. H. The Zebrafish Visual System: From Circuits to Behavior. *Annu. Rev. Vis. Sci.* **5**,
518 269–293 (2019).
519 3. Wei, W. & Feller, M. B. Organization and development of direction-selective circuits in the
520 retina. *Trends Neurosci.* **34**, 638–645 (2011).
521 4. Vaney, D. I., Sivyer, B. & Taylor, W. R. Direction selectivity in the retina: symmetry and
522 asymmetry in structure and function. *Nat. Rev. Neurosci.* **13**, 194–208 (2012).
523 5. Niell, C. M. & Scanziani, M. How Cortical Circuits Implement Cortical Computations: Mouse
524 Visual Cortex as a Model. *Annu. Rev. Neurosci.* **44**, 517–546 (2021).
525 6. Born, R. T. & Bradley, D. Structure and Function of Visual Area MT. *Annu. Rev. Neurosci.* **28**, 157–
526 189 (2005).
527 7. Orban, G. Higher Order Visual Processing in Macaque Extrastriate Cortex. *Physiol. Rev.* **88**, 59–
528 89 (2008).
529 8. Chaplin, T. A., Rosa, M. G. P. & Lui, L. L. Auditory and Visual Motion Processing and Integration
530 in the Primate Cerebral Cortex. *Front. Neural Circuits* **12**, (2018).
531 9. Atkinson, J. The Davida Teller Award Lecture, 2016: Visual Brain Development: A review of
532 "Dorsal Stream Vulnerability"—motion, mathematics, amblyopia, actions, and attention. *J. Vis.*
533 **17**, 26 (2017).
534 10. Hubel, D. H. & Wiesel, T. N. Receptive fields and functional architecture of monkey striate
535 cortex. *J. Physiol.* **195**, 215–43 (1968).
536 11. De Valois, R. L., Yund, E. W. & Hepler, N. The orientation and direction selectivity of cells in
537 macaque visual cortex. *Vision Res.* **22**, 531–544 (1982).
538 12. Dubner, R. & Zeki, S. M. Response properties and receptive fields of cells in an anatomically
539 defined region of the superior temporal sulcus in the monkey. *Brain Res.* **35**, 528–532 (1971).

13. Maunsell, J. & Van Essen, D. C. Functional properties of neurons in middle temporal visual area of the macaque monkey. I. Selectivity for stimulus direction, speed, and orientation. *J. Neurophysiol.* **49**, 1127–1147 (1983).
14. Albright, T. Direction and orientation selectivity of neurons in visual area MT of the macaque. *J. Neurophysiol.* **52**, 1106–30 (1984).
15. Philipp, R., Distler, C. & Hoffmann, K.-P. A motion-sensitive area in ferret extrastriate visual cortex: an analysis in pigmented and albino animals. *Cereb. Cortex* **16**, 779–90 (2006).
16. Lempel, A. A. & Nielsen, K. J. Ferrets as a Model for Higher-Level Visual Motion Processing. *Curr. Biol.* **29**, 179–191 (2019).
17. Li, Y., Fitzpatrick, D. & White, L. E. The development of direction selectivity in ferret visual cortex requires early visual experience. *Nat. Neurosci.* **9**, 676–681 (2006).
18. Clemens, J. M., Ritter, N. J., Roy, A., Miller, J. M. & Van Hooser, S. D. The Laminar Development of Direction Selectivity in Ferret Visual Cortex. *J. Neurosci.* **32**, 18177–18185 (2012).
19. Smith, G. B. *et al.* The development of cortical circuits for motion discrimination. *Nat. Neurosci.* **18**, 252–261 (2015).
20. Chang, J. T. & Fitzpatrick, D. Development of visual response selectivity in cortical GABAergic interneurons. *Nat. Commun.* **13**, 3791 (2022).
21. Li, Y., Van Hooser, S. D., Mazurek, M., White, L. E. & Fitzpatrick, D. Experience with moving visual stimuli drives the early development of cortical direction selectivity. *Nature* **456**, 952–6 (2008).
22. Van Hooser, S. D. *et al.* Initial neighborhood biases and the quality of motion stimulation jointly influence the rapid emergence of direction preference in visual cortex. *J. Neurosci.* **32**, 7258–66 (2012).
23. Ritter, N. J., Anderson, N. M. & Van Hooser, S. D. Visual Stimulus Speed Does Not Influence the Rapid Emergence of Direction Selectivity in Ferret Visual Cortex. *J. Neurosci.* **37**, 1557–1567 (2017).
24. Roy, A., Wang, S., Meschede-Krasa, B., Breffle, J. & Van Hooser, S. D. An early phase of instructive plasticity before the typical onset of sensory experience. *Nat. Commun.* **11**, 11 (2020).
25. Spear, P. D., Tong, L., McCall, M. A. & Pasternak, T. Developmentally induced loss of direction-selective neurons in the cat's lateral suprasylvian visual cortex. *Dev. Brain Res.* **20**, 281–285 (1985).

26. El-Shamayleh, Y., Kiorpes, L., Kohn, A. & Movshon, J. A. Visual Motion Processing by Neurons in Area MT of Macaque Monkeys with Experimental Amblyopia. *J. Neurosci.* **30**, 12198–12209 (2010).
27. Grootel, T. J. V., Raghavan, R. T., Kelly, J. G., Movshon, J. A. & Kiorpes, L. Responses to visual motion of neurons in the extrastriate visual cortex of macaque monkeys with experimental amblyopia. 2024.07.01.601564 Preprint at https://doi.org/10.1101/2024.07.01.601564 (2024).
28. Lempel, A. A. & Nielsen, K. J. Development of visual motion integration involves coordination of multiple cortical stages. *eLife* **10**, e59798 (2021).
29. Bourne, J. A. *et al.* Development of Higher-Level Vision: A Network Perspective. *J. Neurosci.* **44**, e1291242024 (2024).
30. Mazurek, M., Kager, M. & Van Hooser, S. D. Robust quantification of orientation selectivity and direction selectivity. *Front. Neural Circuits* **8**, (2014).
31. Batschelet, E. *Circular Statistics in Biology*. (Academic Press, New York, NY, US, 1981).
32. Chapman, B. & Stryker, M. P. Development of orientation selectivity in ferret visual cortex and effects of deprivation. *J. Neurosci.* **13**, 5251 (1993).
33. Chapman, B., Stryker, M. P. & Bonhoeffer, T. Development of orientation preference maps in ferret primary visual cortex. *J. Neurosci.* **16**, 6443–53 (1996).
34. Bourne, J. A. & Rosa, M. G. P. Hierarchical development of the primate visual cortex, as revealed by neurofilament immunoreactivity: early maturation of the middle temporal area (MT). *Cereb. Cortex* **16**, 405–14 (2006).
35. Warner, C. E., Kwan, W. C. & Bourne, J. A. The Early Maturation of Visual Cortical Area MT is Dependent on Input from the Retinorecipient Medial Portion of the Inferior Pulvinar. *J. Neurosci.* **32**, 17073–17085 (2012).
36. Mundinano, I.-C. *et al.* Transient visual pathway critical for normal development of primate grasping behavior. *Proc. Natl. Acad. Sci.* 201717016 (2018) doi:10.1073/pnas.1717016115.
37. Raiguel, S. E., Xiao, D.-K., Marcar, V. L. & Orban, G. A. Response Latency of Macaque Area MT/V5 Neurons and Its Relationship to Stimulus Parameters. *J. Neurophysiol.* **82**, 1944–1956 (1999).
38. Zhang, B., Smith, E. L. & Chino, Y. M. Postnatal development of onset transient responses in macaque V1 and V2 neurons. *J. Neurophysiol.* **100**, 1476–87 (2008).
39. Raiguel, S. E., Lagae, L., Gulyàs, B. & Orban, G. A. Response latencies of visual cells in macaque areas V1, V2 and V5. *Brain Res.* **493**, 155–159 (1989).

40. Schmolesky, M. T. *et al.* Signal Timing Across the Macaque Visual System. *J. Neurophysiol.* **79**, 3272–3278 (1998).
41. Murphy, A. J., Hasse, J. M. & Briggs, F. Physiological characterization of a rare subpopulation of doublet-spiking neurons in the ferret lateral geniculate nucleus. *J. Neurophysiol.* **124**, 432–442 (2020).
42. Stacy, A. K., Schneider, N. A., Gilman, N. K. & Van Hooser, S. D. Impact of Acute Visual Experience on Development of LGN Receptive Fields in the Ferret. *J. Neurosci.* **43**, 3495–3508 (2023).
43. Khalil, R. & Levitt, J. B. Developmental remodeling of corticocortical feedback circuits in ferret visual cortex. *J. Comp. Neurol.* **522**, 3208–3228 (2014).
44. Krug, K., Akerman, C. J. & Thompson, I. D. Responses of Neurons in Neonatal Cortex and Thalamus to Patterned Visual Stimulation Through the Naturally Closed Lids. *J. Neurophysiol.* **85**, 1436–1443 (2001).
45. Akerman, C. J., Smyth, D. & Thompson, I. D. Visual Experience before Eye-Opening and the Development of the Retinogeniculate Pathway. *Neuron* **36**, 869–879 (2002).
46. Weliky, M., Bosking, W. & Fitzpatrick, D. A systematic map of direction preference in primary visual cortex. *Nature* **379**, 725–728 (1996).
47. Albright, T., Desimone, R. & Gross, C. G. Columnar organization of directionally selective cells in visual area MT of the macaque. *J. Neurophysiol.* **51**, 16–31 (1984).
48. Malonek, D., Tootell, R. B. H. & Grinvald, A. Optical Imaging Reveals the Functional Architecture of Neurons Processing Shape and Motion in Owl Monkey Area MT. *Proc. R. Soc. Lond. B Biol. Sci.* **258**, 109–119 (1994).
49. Pattadkal, J. J., Zemelman, B. V., Fiete, I. & Priebe, N. J. Primate neocortex performs balanced sensory amplification. *Neuron* **112**, 661-675.e7 (2024).
50. Livingstone, M. S., Pack, C. C. & Born, R. T. Two-Dimensional Substructure of MT Receptive Fields. *Neuron* **30**, 781–793 (2001).
51. Thiele, A., Distler, C., Korbmacher, H. & Hoffmann, K.-P. Contribution of inhibitory mechanisms to direction selectivity and response normalization in macaque middle temporal area. *Proc. Natl. Acad. Sci.* **101**, 9810–9815 (2004).
52. Thiele, A., Herrero, J. L., Distler, C. & Hoffmann, K.-P. Contribution of Cholinergic and GABAergic Mechanisms to Direction Tuning, Discriminability, Response Reliability, and Neuronal Rate Correlations in Macaque Middle Temporal Area. *J. Neurosci.* **32**, 16602–16615 (2012).

636 53. Gao, W. J., Newman, D. E., Wormington, A. B. & Pallas, S. L. Development of inhibitory circuitry
637 in visual and auditory cortex of postnatal ferrets: immunocytochemical localization of
638 GABAergic neurons. *J. Comp. Neurol.* **409**, 261–73 (1999).
639 54. Gao, W. J., Wormington, A. B., Newman, D. E. & Pallas, S. L. Development of inhibitory circuitry
640 in visual and auditory cortex of postnatal ferrets: Immunocytochemical localization of
641 calbindin- and parvalbumin-containing neurons. *J. Comp. Neurol.* **422**, 140–157 (2000).
642 55. Mulholland, H. N., Hein, B., Kaschube, M. & Smith, G. B. Tightly coupled inhibitory and
643 excitatory functional networks in the developing primary visual cortex. *eLife* **10**, e72456 (2021).
644 56. Weiskrantz, L., Barbur, J. L. & Sahraie, A. Parameters affecting conscious versus unconscious
645 visual discrimination with damage to the visual cortex (V1). *Proc. Natl. Acad. Sci.* **92**, 6122–
646 6126 (1995).
647 57. Weiskrantz, L. Blindsight revisited. *Curr. Opin. Neurobiol.* **6**, 215–220 (1996).
648 58. Huxlin, K. R. *et al.* Perceptual Relearning of Complex Visual Motion after V1 Damage in
649 Humans. *J. Neurosci.* **29**, 3981–3991 (2009).
650 59. Du, J., Blanche, T. J., Harrison, R. R., Lester, H. A. & Masmanidis, S. C. Multiplexed, High Density
651 Electrophysiology with Nanofabricated Neural Probes. *PLOS ONE* **6**, e26204 (2011).
652 60. nielsenlabmbi. Spike. (2024).
653 61. Brainard, D. H. The Psychophysics Toolbox. *Spat. Vis.* **10**, 433–436 (1997).
654 62. Pelli, D. G. The VideoToolbox software for visual psychophysics: transforming numbers into
655 movies. *Spat. Vis.* **10**, 437–442 (1997).
656 63. Ellaway, P. H. Cumulative sum technique and its application to the analysis of peristimulus
657 time histograms. *Electroencephalogr. Clin. Neurophysiol.* **45**, 302–304 (1978).
658
659
660 **Methods**
661 Animal preparation and surgery
662 All procedures adhered to the guidelines of the national Institute of Health and were approved by
663 the Animal Care and Use Committee at Johns Hopkins University. Experiments were performed in
664 male and female ferrets (*Mustela putoris furo*) aged 29 – 52 days. Animals used in the training
665 experiments were 28- - 33 days old; none of these animals had naturally opened their eyes at the
666 start of the experiment. Recordings were performed in anesthetized ferrets following established
667 procedures described previously [16]. Briefly, animals were anesthetized using isoflurane (during

surgery: 1.5-3%, during recordings: 0.5-2%), and paralyzed using pancuronium bromide (0.15 mg/kg/hr) to prevent eye movements. A range of vital parameters (heart rate, SpO2, EtCO2, EEG) were monitored continuously to ensure adequate anesthetic depth during the experiments. Neosynephrine and atropine were applied to the eyes to retract the nictitating membranes and dilate the pupils. Eyes were then covered with contact lenses. Craniotomies were made over V1 and PMLS, targeting related visual field positions.

Extracellular recordings and extraction of neural responses

Neural responses were recorded using multichannel silicon probes obtained from the Masmanidis lab at UCLA [59], plated with gold to reach impedances around 150-300 kΩ. Signals from one or two probes were recorded with a RHD2000 amplifier (intan Technologies) using sampling rates of 20-30 kHz. Data was filtered offline between 250 Hz and 5kHz. Based on these filtered signals, two types of neural responses were extracted. Single units were isolated using a custom-written processing pipeline in Matlab (MathWorks) for manual spike sorting (available on github [60]). In this pipeline, detection thresholds were first set manually for each recording channel based on noise levels. Spikes detected on channels with distances up to 50um that occurred within +/- 0.2 ms of each other were assigned to the channel with the largest energy and eliminated from other channels. Spikes were then manually clustered using multiple waveform characteristics like through amplitude, energy, or trough-peak amplitude, as well as recording position on the probe (determined as center-of-mass of the spike energy or trough amplitude computed across neighboring probe channels). Quality of isolation was confirmed by analyzing inter-spike intervals and eliminating any units with intervals below 1.2 ms. Multi-unit signals were extracted by first applying an automatically computed detection threshold to every channel. The threshold was set to 4 times the standard deviation of each channel's bandpass-filtered signal, using the median absolute deviation scaled for a normal distribution to estimate the standard deviation. Again, events detected within +/-0.2 ms on channels within 50 um were assigned only to the channel with the largest energy. No further spike sorting was performed on this multi-unit signal.

Visual stimuli and experiment design

Visual stimulus generation: Stimuli were generated using the Psychophysics Toolbox extension to Matlab [61,62] and displayed on a 23 inch LCD monitor with a refresh rate of 120 Hz, placed 20 – 35 cm in front of the ferret. The monitor was gamma corrected using a SpectraScan 655 (PhotoResearch).

Stimuli for selectivity measurements: Except for the stimulation blocks of the exposure paradigm, all data was collected by presenting gratings drifting in 12 or 16 directions. Gratings were shown full-field (about 65 x 50 deg), with the exception of 3 experiments that also presented an additional smaller size. For those experiments, only the full-field data was analyzed. With the exception of 2 experiments (ages P45 & P48) that used a sine-wave profile, gratings were square-wave gratings shown at 100% contrast. Spatial and temporal frequency were optimized per recording, and ranged between 0.01 – 0.1 cyc/deg and 1 - 6 cyc/s, respectively. In addition to the different directions, each experiment also contained a blank condition. All conditions were shown in a pseudo-random sequence with 5 repetitions per condition. Within each condition, each presentation of a stimulus was preceded and followed by presentation of a gray screen of equal luminance. Stimuli were shown for 1 s, with inter-stimulus intervals of 3 - 10 s (longer intervals were needed for the youngest animals in which adaptation to the stimulus is more pronounced).

Stimuli during training paradigm: For the animals exposed to drifting or flashing stimuli, we presented full-field, square-wave gratings during the stimulation blocks. Stimuli were shown for 5 s, with 10 s inter-stimulus intervals. Spatial frequency was again adjusted based on responses in an individual animal, and ranged between 0.05 – 0.08 cyc/deg for both groups. For the drifting gratings, temporal frequency ranged between 3 – 6 cyc/deg. Drifting gratings were always shown at 100% contrast. For the flashing gratings, we modulated contrast between 0 and 100% (no contrast reversal) using a sinusoidal function with a temporal frequency of 3 Hz.

Data analysis

<u>Inclusion criteria and data set size</u>

For the analysis of SU responses, neural responses to every stimulus were calculated as the firing rate during the stimulus presentation period (1s long) minus the firing rate during the last second of the pre-stimulus period. SU needed to pass two criteria to be included in the analyses. First, we computed an ANOVA across the responses in all stimulus conditions, including the blank. Only SU with $p<.05$ for the ANOVA were included. Additionally, the average firing rate for the best condition had to exceed 0 Hz.

For the analysis of response latency using MU data, we used the same approach to test for visual responsiveness (ANOVA for the baseline-corrected firing rates with $p<.05$, firing rate for best

stimulus > 0Hz). Additionally, the data set as limited to simultaneous recordings from V1 and PMLS. This MU data set includes the same data used for SU analysis of DS development, but contains additional data in which no SU could be isolated or in which no SU passed the criteria.

MU data was also used to analyze the effects of the exposure paradigm. In this case, the long duration of the experiments generally made responses more variable, which required an adjustment in the inclusion criteria. For these data, we tested for visual responsiveness by comparing the stimulus-evoked firing rates (not baseline corrected) to the spontaneous activity during the 1s preceding each stimulus presentation (blanks were excluded from this analysis). MU with $p<.05$ and with responses to the preferred stimulus exceeding 0Hz were included in subsequent analyses. Further, data were restricted to experiments in which visually responses sites could be identified before and after the exposure. This meant that for a few animals only PMLS data (1 animal in the flashing and gray cohort each) or V1 data (1 animal in the gray cohort) was available. These cases were eliminated when comparing exposure effect sizes between V1 and PMLS (Fig, 4E, G). Finally, no responsiveness criterion was applied to the MU collected during the exposure blocks. The resulting number of animals and neurons for normal development and exposure experiments are listed in Table 1.

Measurements of DS and OS

DS was quantified using 2 metrics, L_{dir} and DSI. L_{dir} was computed as [30]

$$L_{dir} = \left|\frac{\sum_k R(\theta_k)\exp(i\theta_k)}{\sum_k R(\theta_k)}\right|,$$

where $R(\theta_k)$ represents the response to angle θ_k. DSI was computed as

$$DSI = 1 - \frac{R(N)}{R(P)},$$

where R(P) is the response to the preferred and R(N) the response to the null direction. Matching metrics were computed for OS:

$$L_{ori} = \left|\frac{\sum_k R(\theta_k)\exp(2i\theta_k)}{\sum_k R(\theta_k)}\right| \text{ and } OSI = 1 - \frac{R(O)}{R(P)},$$

with R(O) the response to the orthogonal direction.

Normalized DS and OS metrics

To compare development of DS and OS across areas without the effects of different selectivity levels in adults, normalized L_{dir} and L_{ori} values were computed. For this analysis, SU were first

762 binned into 6 age windows, P29-30, P31-32, P33-34, P35-36, P37-39, P44-45. The age window from
763 P37-39 was expanded to include a single V1 animal at P39. We then computed the average L_{dir} value
764 for the first and last bin. All L_{dir} values were then normalized by computing

765 $$norm\ L_{dir} = \frac{L_{dir} - \bar{L}_{dir,EO}}{\bar{L}_{dir,adult} - \bar{L}_{dir,EO}}$$

766 where $\bar{L}_{dir,EO}$ refers to the average L_{dir} value in the first age group around eye opening, and $\bar{L}_{dir,adult}$
767 to the average value in the last, adult group. The same analysis was repeated to compute
768 normalized L_{ori} values.
769
770 Measurements of latency
771 Latency was computed for each MU site based on the responses to its best condition. Latencies
772 were computed using cumulative sum analysis [63] using similar statistical criteria as used previously
773 for primate MT neurons [37]. First, responses were binned into 10 ms bins to first compute the PSTH.
774 Second, mean and standard deviation of the baseline rate were computed for the 1 s baseline
775 preceding stimulus onset, and the baseline mean was subtracted from the PSTH before computing
776 the cumulative sum of the PSTH. The latency was then taken as the first bin after stimulus onset in
777 which the cumulative PSTH was larger than two standard deviations (of the baseline rate), followed
778 by 2 increasing bins. For the analysis of latency development in shorter age windows, data from V1
779 and PMLS was binned into the following age windows: P29-30, P31-32, P33-34, P35-36, P37-39,
780 P42-52. These are the same age windows used for the normalized DS and OS metric, but the adult
781 window was expanded to include more animals in which paired V1 and PMLS data were available.
782
783 Analysis of MU responses in stimulation blocks
784 To analyze response patterns during the stimulation blocks, responses were computed during the 5
785 s of stimulus presentation. To compute average rate, the firing rate was computed for each 5 s
786 stimulus presentation period, baseline corrected by the firing rate in the preceding 2 s baseline
787 period, and averaged across all stimulus presentation periods. To compute peak rate and response
788 duration, we first computed the PSTH across all stimulus presentation periods using 10 ms bins.
789 The peak rate was set to the maximum of the PSTH, baseline corrected as before. Duration was
790 quantified as the number of bins during the stimulus presentation exceeding the baseline rate by 2
791 standard deviations, converted to seconds. Finally, all metrics were averaged across all blocks for
792 each channel. This assumes that there are no significant movements of the probe throughout the

experiment. Treating each block as an independent measurement (no averaging across blocks) does not affect the results.

Statistics

For all normal development data, we first used an ANOVA or Kruskall-Wallis test to establish high-level differences between groups or areas (see Tables 2-6). Post-hoc tests (where justified) were then performed using Wilcoxon rank-sum tests. The outcome of all statistical tests is listed in Tables 2-6. For the training data, we performed two different kinds of analyses. First, we compared before and after training data, combined across all animals, for each area using a rank-sum test. Second, we fit the L_{dir} MU data with a LME model (lmefit, Matlab), with training phase (before/after exposure to the stimulus) as fixed effect and by-animal random intercepts and slopes. We compared this model against one omitting the by-animal random slopes; in most instances, the model including random slopes outperformed the one without (based on likelihood-ratio comparisons), so for consistency, we used the model with random slopes in all cases. Models were fit using maximum likelihood estimation, and the significance of the fixed effect was assessed using an ANOVA. Effect size per animal was computed as the sum of the fixed effect slope and the random, per-animal slope.

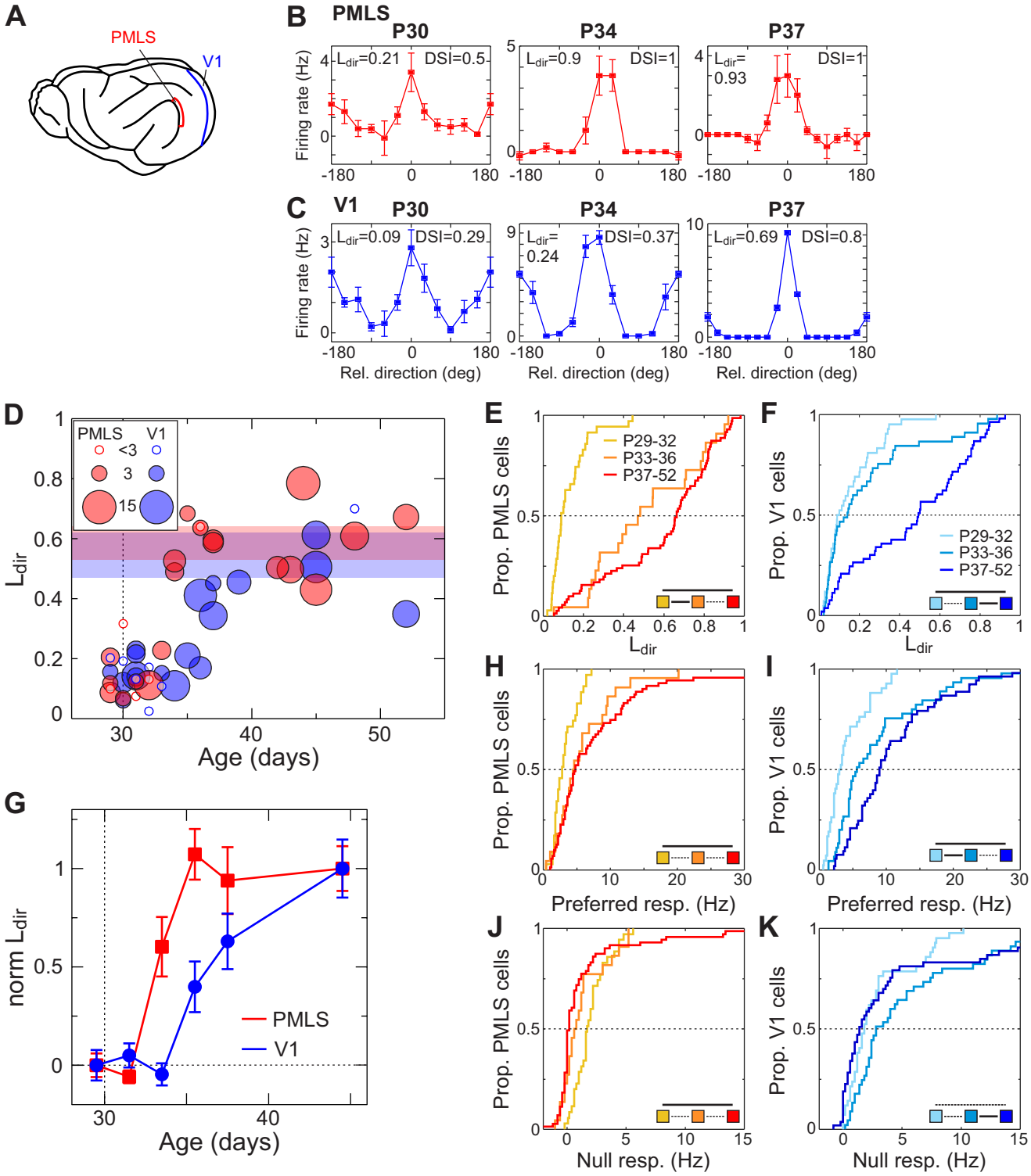
A
PMLS
V1
B
PMLS
P30
P34
P37
Firing rate (Hz)
Ldir=0.21
DSI=0.5
Ldir=0.9
DSI=1
Ldir=
0.93
DSI=1
C
V1
P30
P34
P37
Ldir=0.09
DSI=0.29
Ldir=
0.24
DSI=0.37
Ldir=0.69
DSI=0.8
Rel. direction (deg)
D
PMLS
V1
<3
3
15
Ldir
Age (days)
E
P29-32
P33-36
P37-52
Prop. PMLS cells
Ldir
F
Prop. V1 cells
G
norm Ldir
PMLS
V1
Age (days)
H
Prop. PMLS cells
Preferred resp. (Hz)
I
Prop. V1 cells
J
Null resp. (Hz)
K

Figure 1

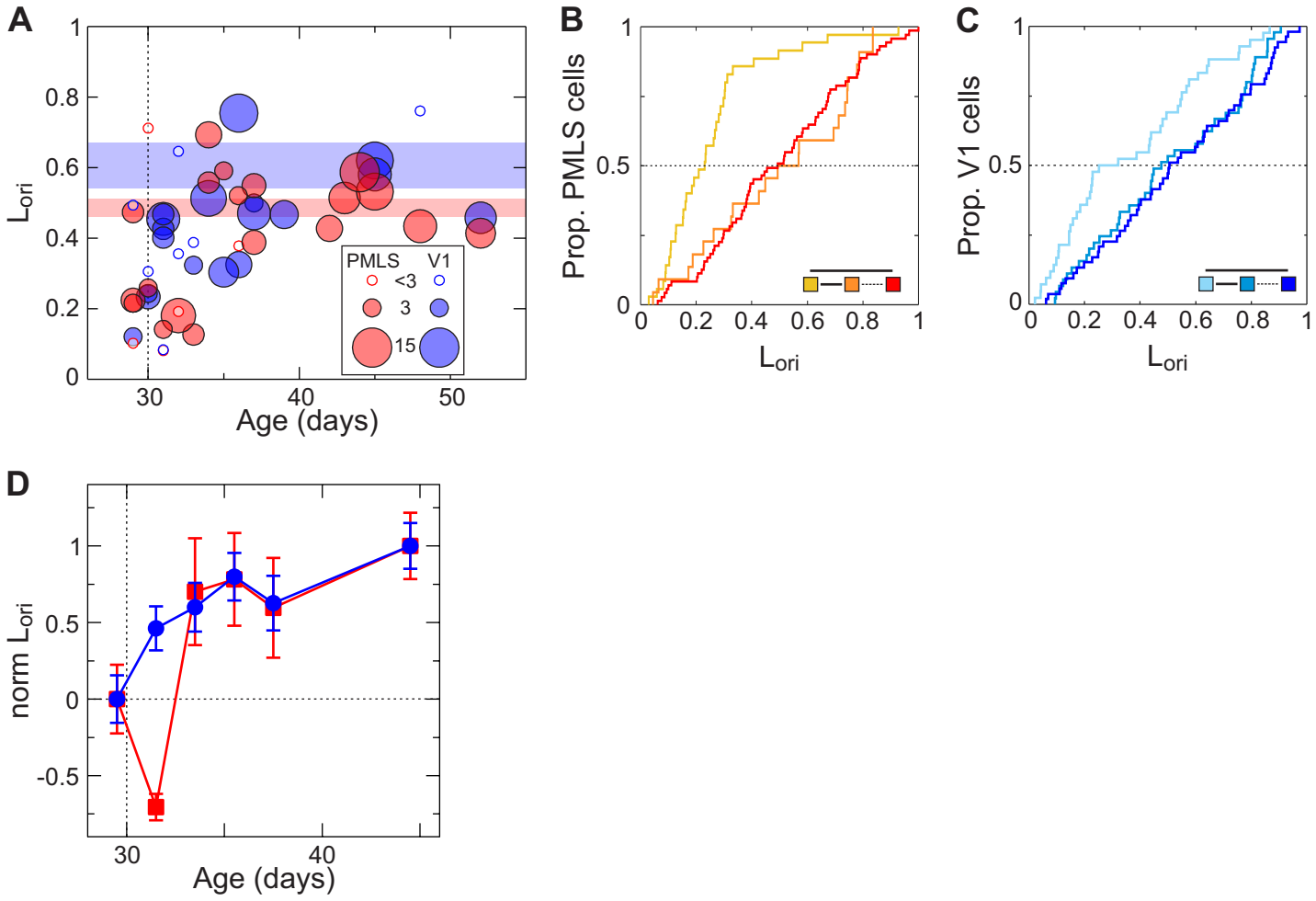
A
B
C
D
Lori
Age (days)
PMLS
V1
<3
3
15
Prop. PMLS cells
Prop. V1 cells
norm Lori

Figure 2

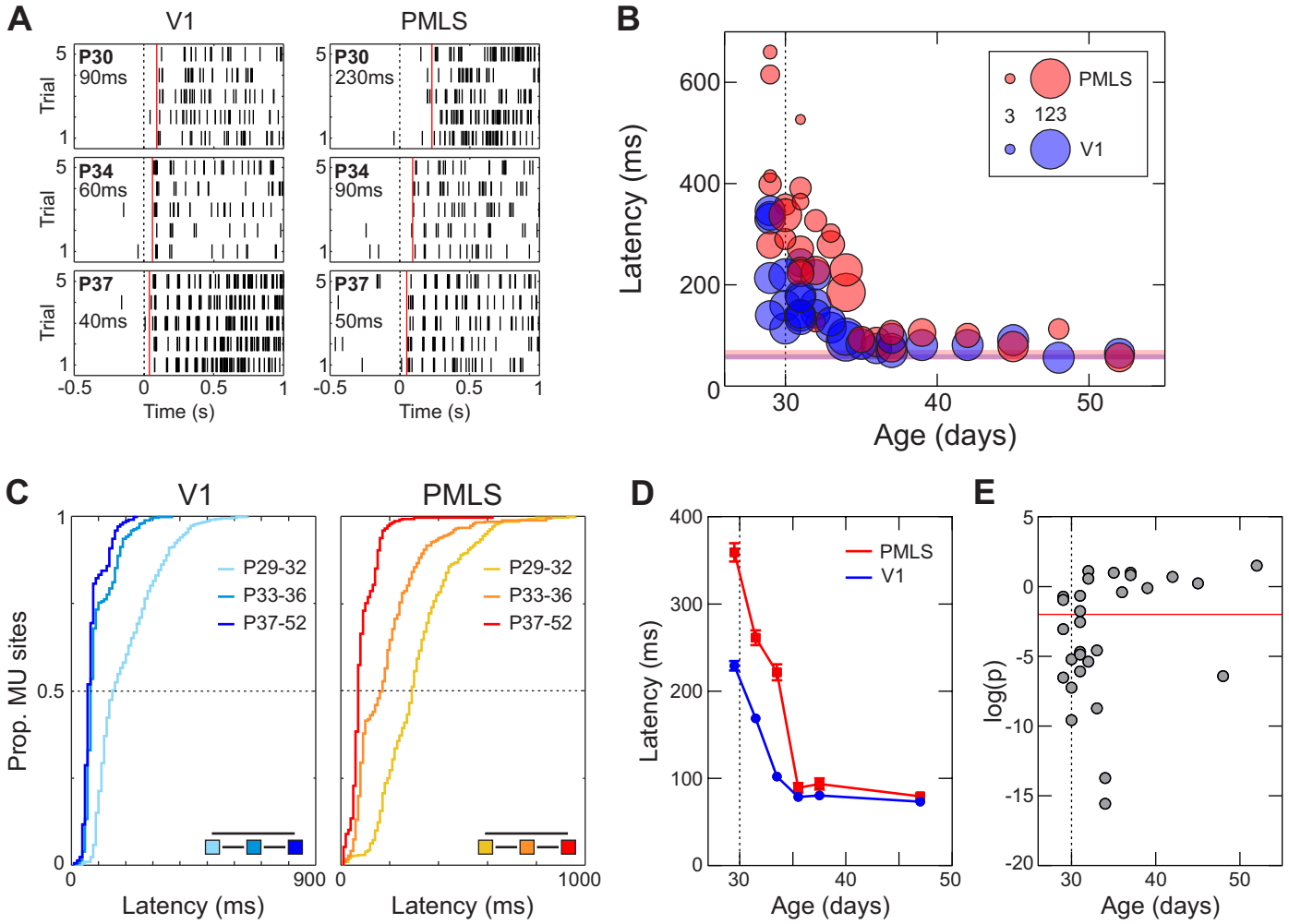
A
V1
PMLS
P30
90ms
P30
230ms
P34
60ms
P34
90ms
P37
40ms
P37
50ms
Trial
Time (s)
B
Latency (ms)
Age (days)
PMLS
3 123
V1
C
V1
PMLS
Prop. MU sites
P29-32
P33-36
P37-52
Latency (ms)
D
Latency (ms)
Age (days)
PMLS
V1
E
log(p)
Age (days)

Figure 3

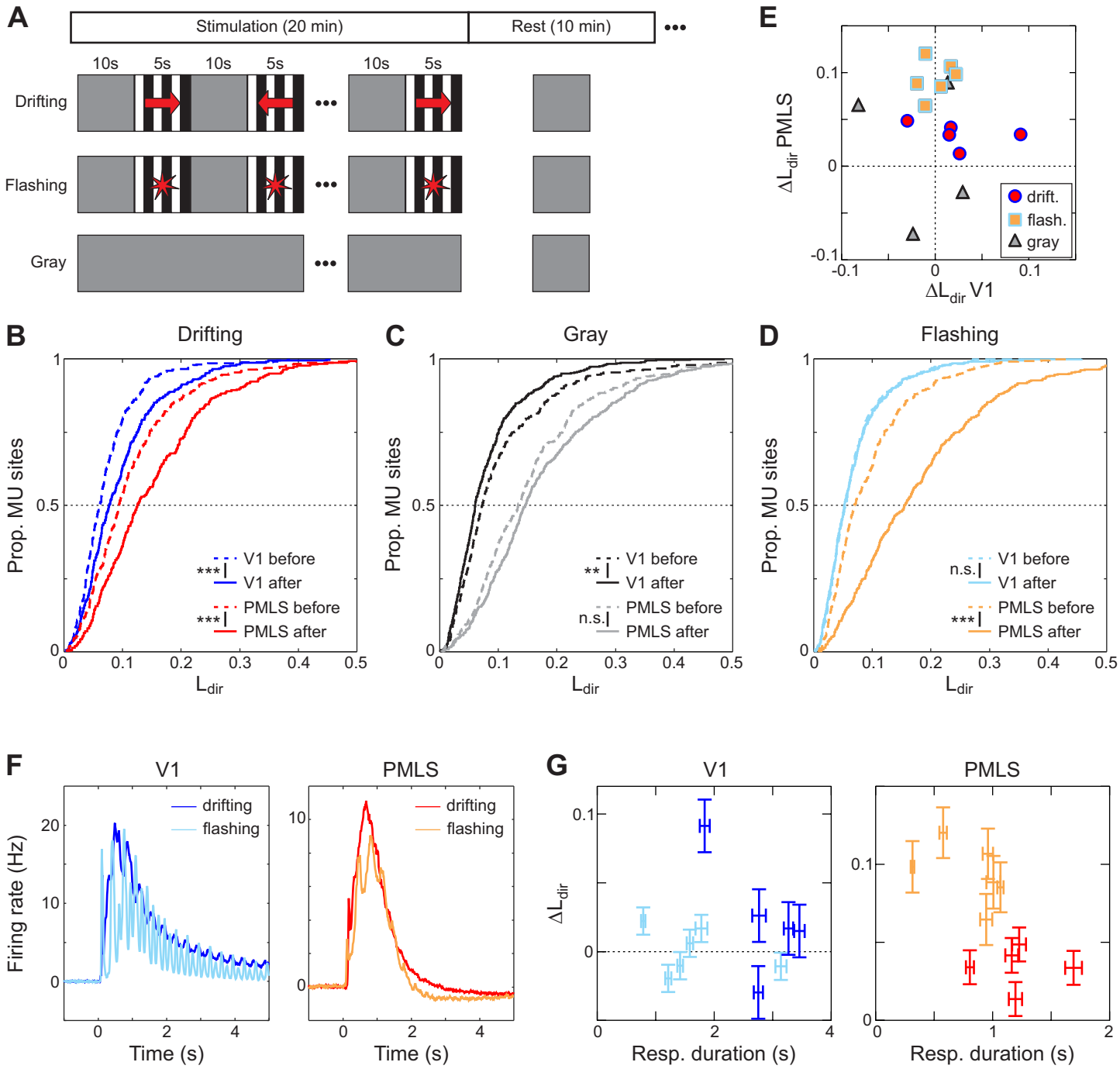
A
Stimulation (20 min)
Rest (10 min)
10s
5s
Drifting
Flashing
Gray
E
ΔL_dir PMLS
ΔL_dir V1
drift.
flash.
gray
B
Drifting
C
Gray
D
Flashing
Prop. MU sites
L_dir
V1 before
V1 after
PMLS before
PMLS after
***
**
n.s.
F
V1
PMLS
drifting
flashing
Firing rate (Hz)
Time (s)
G
ΔL_dir
Resp. duration (s)

Figure 4

Tables

Figure	Exp. Group	N Animals	N SU/MU
1D & 2A, S1A & B	PMLS	24	128 (SU)
1D & 2A, 3, S1A & B	V1	25	140 (SU)
1E, H & J, 2C, S1C & D	PMLS, P29-32	10	35 (SU)
1E, H & J, 2C, S1C & D	PMLS, P33-36	6	22 (SU)
1E, H & J, 2C, S1C & D	PMLS, P37-52	8	71 (SU)
1F, I & K, 2D, S1E & F	V1, P29-32	12	42 (SU)
1F, I & K, 2D, S1E & F	V1, P33-36	6	45 (SU)
1F, I & K, 2D, S1E & F	V1, P37-52	7	53 (SU)
1G & 2B, S2A	PMLS	2-6	8-28 per age group (SU)
1G & 2B, S2A	V1	2-7	15-23 per age group (SU)
3B, E	PMLS	30	1065 (MU)
3B, E	V1	30	1904 (MU)
3C	PMLS, P29-32	17	439 (MU)
3C	PMLS, P33-36	6	337 (MU)
3C	PMLS, P37-52	7	289 (MU)
3C	V1, P29-32	17	1006 (MU)
3C	V1, P33-36	6	464 (MU)
3C	V1, P37-52	7	436 (MU)
3D	PMLS	2-9	95-242 per age group (MU)
3D	V1	2-9	121-517 per age group (MU)
4B	PMLS, before	5	297 (MU)
4B	PMLS, after	5	297 (MU)
4B	V1, before	5	320 (MU)
4B	V1, after	5	312 (MU)
4C	PMLS, before	7	404 (MU)
4C	PMLS, after	7	380 (MU)
4C	V1, before	6	382 (MU)
4C	V1, after	6	383 (MU)
4D	PMLS, before	5	344 (MU)
4D	PMLS, after	5	463 (MU)
4D	V1, before	5	278 (MU)
4D	V1, after	5	467 (MU)
4E, G	PMLS	4-6	47-237 per animal (MU)
4E, G	V1	4-6	31-114 per animal (MU)
4F	V1, drifting	5	320 (MU)
4F	V1, flashing	6	384 (MU)
4F	PMLS, drifting	5	319 (MU)
4F	PMLS, flashing	6	384 (MU)
4G	V1, resp. dur.	5-6	64 per animal (MU)
4G	PMLS, resp. dur.	5-6	63-64 per animal (MU)

Table 1: Data set sizes for all figures and analyses

Metric	Group	Test	PMLS p value	PMLS other	V1 p value	V1 other
L_{dir}	All age groups	Kruskall-Wallis	<0.001	X(2)=56.5	<0.001	X(2)=30.2
L_{dir}	P29-32 vs P33-36	Rank sum	<0.001		0.3	
L_{dir}	P29-32 vs P37-52	Rank sum	<0.001		<0.001	
L_{dir}	P33-36 vs P37-52	Rank sum	0.2		<0.001	
Pref.	All age groups	Kruskall-Wallis	<0.001	X(2)=14.5	<0.001	X(2)=34.3
Pref.	P29-32 vs P33-36	Rank sum	0.02		<0.001	
Pref.	P29-32 vs P37-52	Rank sum	<0.001		<0.001	
Pref.	P33-36 vs P37-52	Rank sum	0.5		0.03	
Null	All age groups	Kruskall-Wallis	<0.001	X(2)=21	0.008	X(2)=9.6
Null	P29-32 vs P33-36	Rank sum	0.02		0.01	
Null	P29-32 vs P37-52	Rank sum	<0.001		0.6	
Null	P33-36 vs P37-52	Rank sum	0.5		0.006	

Table 2: Statistics for Figs. 1E, F, H-K

Metric	Group	Test	p value	Other
Norm. L_{dir}	V1 vs PMLS	ANOVA: area, age	Age: <0.001 Area: <0.001 IA: 0.003	Age: F(3)=19.6 Area: F(1)=18.1 IA: F(3)=4.9
Norm. L_{dir}	V1 vs PMLS, P31-32	Rank sum	0.52	
Norm. L_{dir}	V1 vs PMLS, P33-34	Rank sum	<0.001	
Norm. L_{dir}	V1 vs PMLS, P35-36	Rank sum	0.02	
Norm. L_{dir}	V1 vs PMLS, P37-39	Rank sum	0.14	

Table 3: Statistics for Figs. 1G (IA: Interaction)

Metric	Group	Test	PMLS p value	PMLS other	V1 p value	V1 other
L_{ori}	All age groups	Kruskall-Wallis	<0.001	X(2)=24.9	0.004	X(2)=10.9
L_{ori}	P29-32 vs P33-36	Rank sum	<0.001		0.009	
L_{ori}	P29-32 vs P37-52	Rank sum	<0.001		0.002	
L_{ori}	P33-36 vs P37-52	Rank sum	0.9		0.6	

Table 4: Statistics for Figs. 2B & C

Metric	Group	Test	p value	Other
Norm. L_{ori}	V1 vs PMLS	ANOVA: area, age	Age: <0.001 Area: 0.07 IA: 0.003	Age: F(3)=8.9 Area: F(1)=3.4 IA: F(3)=4.8
Norm. L_{ori}	V1 vs PMLS, P31-32	Rank sum	<0.001	
Norm. L_{ori}	V1 vs PMLS, P33-34	Rank sum	0.6	
Norm. L_{ori}	V1 vs PMLS, P35-36	Rank sum	0.95	
Norm. L_{ori}	V1 vs PMLS, P37-39	Rank sum	0.9	

Table 5: Statistics for Figs. 2D (IA: Interaction)

Metric	Group	Test	PMLS p value	PMLS other	V1 p value	V1 other
Latency	All age groups	Kruskall-Wallis	<0.001	X(2)=468.3	<0.001	X(2)=816.4
Latency	P29-32 vs P33-36	Rank sum	<0.001		<0.001	
Latency	P29-32 vs P37-52	Rank sum	<0.001		<0.001	
Latency	P33-36 vs P37-52	Rank sum	<0.001		<0.001	

Table 6: Statistics for Fig. 3C

Group	Test	p value	Other
All age groups	ANOVA: area, age	Area: <0.001 Age: <0.001 IA: <0.001	Area: F(1)=228.4 Age: F(5)=354.2 IA: F(5)=35.8
V1 vs PMLS, P29-30	Rank sum	<0.001	
V1 vs PMLS, P31-32	Rank sum	<0.001	
V1 vs PMLS, P33-34	Rank sum	<0.001	
V1 vs PMLS, P35-36	Rank sum	0.05	
V1 vs PMLS, P37-39	Rank sum	0.03	
V1 vs PMLS, P40-52	Rank sum	0.02	

Table 7: Statistics for Fig. 3D (IA: interaction)

Training stim.	Parameter	V1	PMLS
Drifting	Phase: Estimate	Full data: 0.02 Reduced data: 0.04	0.03
Drifting	Phase: p value	Full data: 0.2 Reduced data: 0.009	<0.001
Drifting	Slope per animal	0.02, 0.09, -0.03, 0.02, 0.03	0.04, 0.03, 0.05, 0.03, 0.01
Gray	Phase: Estimate	-0.03	0.01
Gray	Phase: p value	0.2	0.7
Gray	Slope per animal	-0.1, 0.01, -0.02, 0.03, -0.08	0.09, -0.07, -0.002, -0.03, 0.07
Flashing	Phase: Estimate	0.0008	0.09
Flashing	Phase: p value	0.9	<0.001
Flashing	Slope per animal	-0.02, 0.02, 0.02, -0.01, -0.01, 0.006	0.09, 0.11, 0.10, 0.08, 0.12, 0.06, 0.09

Table 8: LME results for Fig. 4B-D. Phase: Slope for the fixed effect training phase (before/after); slope: fixed effect slope + random effect slope per animal.

Metric	Group	Test	PMLS p value	PMLS other	V1 p value	V1 other
DSI	All age groups	Kruskall-Wallis	<0.001	X=38.7	<0.001	X=27.3
DSI	P29-32 vs P33-36	Rank sum	<0.001		0.6	
DSI	P29-32 vs P37-52	Rank sum	<0.001		<0.001	
DSI	P33-36 vs P37-52	Rank sum	0.2		<0.001	
OSI	All age groups	Kruskall-Wallis	<0.001	X=19.7	0.03	X=6.9
OSI	P29-32 vs P33-36	Rank sum	0.001		0.01	
OSI	P29-32 vs P37-52	Rank sum	<0.001		0.05	
OSI	P33-36 vs P37-52	Rank sum	0.8		0.6	

Table 9: Statistics for Figs. S1C-F

Area	Metric	Test	p value	Other
V1 & PSS	Peak rate	ANOVA: area, stimulus type	Area: <0.001 Stim type: 0.12 IA: 0.3	Area: F(1)=282.4 Stim type: F(1)=2.4 IA: F(1)=1.2
V1 & PMLS	Response duration	ANOVA: area, stimulus type	Area: <0.001 Stim type: <0.001 IA: <0.001	Area: F(1)=9733.9 Stim type: F(1)=400.4 IA: F(1)=93.7
V1 & PMLS	Average rate	ANOVA: area, stimulus type	Area: <0.001 Stim type: <0.001 IA: <0.001	Area: F(1)=312.0 Stim type: F(1)=63.7 IA: F(1)=18.5
V1	Response duration	Rank sum	<0.001	
V1	Average rate	Rank sum	<0.001	
PMLS	Response duration	Rank sum	<0.001	
PMLS	Average rate	Rank sum	<0.001	

Table 10: Statistics for Fig. S4 (IA: interaction). All rank-sum tests compare drifting versus flashing gratings.